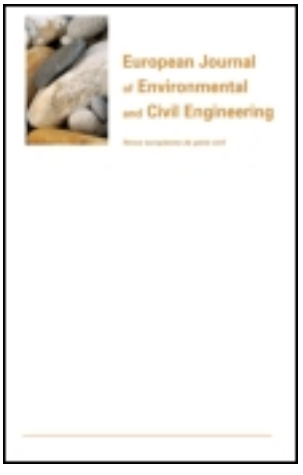

European Journal of Environmental and Civil Engineering
Publication details, including instructions for authors and subscription information:
http://www.tandfonline.com/loi/tece20

Elasto-plastic analysis of the pressuremeter test in granular soil - part I: theory

J. Monnet [a]
[a] Joseph Fourier University, Grenoble, France
Published online: 26 Apr 2012.

To cite this article: J. Monnet (2012): Elasto-plastic analysis of the pressuremeter test in granular soil - part I: theory, European Journal of Environmental and Civil Engineering, 16:6, 699-714

To link to this article: http://dx.doi.org/10.1080/19648189.2012.675171

European Journal of Environmental and Civil Engineering
Vol. 16, No. 6, June 2012, 699–714

Elasto-plastic analysis of the pressuremeter test in granular soil – part I: theory

J. Monnet*

Joseph Fourier University, Grenoble, France

In this first paper, part I, we present the elasto-plastic theory for expansion of pressuremeters in granular soil. This theory allows determination of the behaviour of the granular soil around the pressuremeter with only four mechanical parameters. It is compared with previous theory on the dataset of the pressuremeter test on Ticino sand. In the second paper, part II, we present a numerical analysis of the theoretical conventional limit pressure compared with the results of the Mohr–Coulomb non-standard model used by the Plaxis finite element program. The theoretical evolution of the conventional limit pressure as a function of the variation of each parameter shows a correct agreement with the numerical results. Conclusions are drawn on the influence of these parameters on the pressuremeter results.

Dans un premier article, partie I, nous présentons la théorie élasto-plastique de l'expansion de la sonde dans le sol granulaire. Cette théorie permet de déterminer le comportement du sol granulaire autour du pressiomètre avec seulement quatre paramètres mécaniques. Nous comparons ensuite ses résultats à ceux de théories plus anciennes pour l'étude des essais pressiométriques réalisés dans le sable de Ticino. Dans un second article, partie II, nous réalisons l'étude analytique de l'évolution de la pression limite donnée par cette théorie et nous la comparons à la valeur numérique trouvée avec le logiciel Plaxis L'évolution de la pression limite en fonction de la variation de chacun de ses paramètres montre un accord raisonnable avec les résultats numériques de Plaxis. Nous concluons sur l'importance relative de ces paramètres sur la pression limite.

Keywords: Pressuremeter; analysis; granular soil; limited pressure; finite element; validation

Mots-clés: .pressiomètre; analyse; sol granulaire; pression limite; éléments finis; validation

1. Introduction

The pressuremeter is a well-known apparatus and is widely used for foundation engineering (Amar, Clarke, & Gambin, 1991; Clarke, 1996; Clough, Briauld, & Hughes, 1990; Gambin, 1990; Ménard, 1975). A general presentation of this technique can be found in Cassan (2005) and Dalton (2005). Its use, however, often relies on a set of empirical rules (DTU 13.12, 1988; French Standard NF P 94-110, 2000; French Standard P 94-250-1, 1996) for the design of foundation. But a pressuremeter test may also be considered as an *in situ* shearing test, to measure soil properties using theories of cavity expansion (Monnet & Allagnat, 2006; Monnet, Allagnat, Teston, Billet, &

*Email: jmonnet@ujf-grenoble.fr

ISSN 1964-8189 print/ISSN 2116-7214 online

http://dx.doi.org/10.1080/19648189.2012.675171
http://www.tandfonline.com

Baguelin 2006; Durkee, Langer, Hughes, & Smith, 2005; Fahey, 2005; Monnet & Allagnat, 2002; Monnet & Khlif 1994; Silvestri, 2001). The main interest of this approach is the measurement of soil deformability and shear resistance *in situ*, performed in any type of soil, without sampling. This avoids problems of grain size distribution and disturbance of the soil after sampling, often encountered in samples used for laboratory testing.

2. Behaviour of granular soil around the pressuremeter

Recent developments in pressuremeter interpretation show that the volume changes due to compression and dilation must be taken into account. Three different approaches can be used:

- The first approach is theoretical and uses a constant dilatancy angle Ψ function of the critical state friction angle Φ_{cv} and of the friction angle Φ'. The important work of Hughes, Wroth, and Windle (1977) assumes a dilatancy with the Rowe (1969) theory and a plane strain deformation of the soil in the horizontal plane. The vertical stress is assumed to be the intermediate stress and no plastic vertical strains are allowed. They found the logarithmic expression of the pressuremeter expansion curve with an unknown constant. Later, Jewell, Fahey, and Wroth (1980) used a pressuremeter in a calibration chamber, with various boundary conditions. They found that there is a possibility of a failure between the circumferential and vertical axis, which violates the plane strain vertical hypothesis from Hughes et al. (1977). This observation was also made by Fahey (1986), who measured a variation of the vertical stress. Fahey found that the constant dilatancy angle Ψ is validated by experiments. He determined an expression of the constant in Hughes et al. (1977) theory. Carter, Booker, and Yeung (1986) used small strain theory for the expansion of a cylindrical or spherical cavity. They assumed vertical plane strain condition with no plasticity along the vertical axis.
- The second approach is a derivation of the pressuremeter curve to find the shear-stress shear-strain relation from the pressuremeter measurement. The first analysis was carried out by Baguelin, Jezequel, Le Mee, and Le Mehauté (1972). Juran and Beech (1986) and Juran and Mahmoodzadegan (1989) used a non-associated elasto-plastic flow rule condition in the horizontal plane, with vertical plane strain condition. They derived the pressuremeter curve with the help of six constitutive parameters to find the shearing stress of the soil and to determine the friction angle Φ. Recently, Silvestri (2001) assumed a large strain in the horizontal plane, with plane strain along the vertical direction, and the Rowe dilatancy relation. He assumed no elastic strain in the test, and a plastic deformation at the very beginning of the test, which is not confirm by experiments (Fahey & Carter, 1992). He carried out the derivation of the pressuremeter expansion curve to find the shear strain of the soil by the numerical resolution of an integrative relation. He used a numerical process to find the stress path followed along the pressuremeter test, which allows deduction of friction angle Φ. There is no analytical relation for the pressuremeter curve. Silvestri (2001) used a plane strain assumption along the vertical axis. He derived the pressuremeter curve to obtain an estimation of the shearing strength. The use of the Rowe (1962) dilatancy relation allows definition of the stress–strain relation at the borehole wall, and the friction angle of the soil.

- The third approach is numerical has undergone considerable development. It can be organised around two different tools, the finite element method and the neuronal method. The development of the finite element program allows numerical simulation of the pressuremeter expansion which can be compared with experiments. Cambou and Bahar (1993) used seven mechanical parameters in the plane strain condition along the vertical axis. In such a case, four parameters should be assumed from experiments on the soil tested and the three remaining parameters are determined by best fitting the experimental curve. The finite element study of Fahey and Carter (1992) required nine mechanical parameters to describe the elastic and plastic deformations of the test in plane strain condition. They concluded that the best fit between experiments and numerical results is not linked to a unique set of parameters and requires complementary results (seismic penetration test). Obrzud, Vulliet, and Truty (2009) and Levasseur, Malecot, Boulon, and Flavigny (2010) stated that it is possible to use a neuronal network to estimate the model parameters of a finite element program. The discrepancy between the numerical and the experimental results is reduced by an iterative optimisation of the parameters.

This paper can be considered as a development of the first theoretical approach, and a contribution to improving the theory, using theoretical expressions of the vertical equilibrium of the soil, yielding along the vertical axis as observed by Jewell et al. (1980) but not modelled previously. Another interest of this theoretical analysis is its ability to describe the pressuremeter test with only a few constitutive parameters (G, Φ and Φ_μ) and the condition of stress (σ_z and K_0), when numerical analysis needs many mechanical parameters, which cannot be precisely fitted. We use elasto-plasticity as the general frame of this study, due to its ability to cover the total range from small elastic displacements at low levels of shearing to large plastic displacements at high levels of shearing linked to the conventional limit pressure. The theoretical analysis assumes small deformations, leading to an analytical formulation, whereas large deformations should be more appropriate for the conventional limit pressure; however, this limitation does not change the mechanical parameters involved in the behaviour of the soil. Furthermore the conventional limit pressure is defined by a volume probe which is twice the initial value. This condition leads to a circumferential strain of $\sqrt{2} - 1$. With logarithmic definition of large strain, this deformation is equal to 0.346, which is 19% smaller than the small deformation value. This difference is considered to be acceptable, given the simplification of the theory.

2.1. Hypothesis

Following Baguelin, Jezequel, and Shields (1978), we assume a drained test with an elastic behaviour at low level of shear with two elastic parameters, the Young modulus E and the Poisson ratio ν. Numerical results with the Cambou model (Cambou & Bahar, 1993) show that the test should be assumed as a drained test with permeability higher than 10^{-8} m s^{-1} Thus pore pressure is constant along the radius, regardless of the deformation.

Like Monnet (1990), Yu and Houlsby (1991), Allouani, Cambou, and Dubujet (1995), Cambou and Bahar (1993) and Bahar, Cambou, Labanieh, and Foray (1995) we assume a non associated plasticity for a higher level of shear and a drained pressuremeter test. The non-associated flow rule is function of the unknown scalar ξ, the plastic potential $H(\sigma')$ (Equation (1)) and the dilatancy angle Ψ (Equation (2)). The

Mohr–Coulomb failure criterion is Equation (3), with the main direction 1, which is along the radius, the minor direction 3, which is either along the circumferential or the vertical direction, and the intermediate direction 2, which is either the vertical or the circumferential direction and σ'_1, σ'_2, σ'_3 the effective principal stress

$$H(\sigma') = (\sigma'_1 - \sigma'_3) - \sin\Psi.(\sigma'_1 + \sigma'_3) \tag{1}$$

$$d\vec{\varepsilon}^p = \xi(1 - \sin\psi, \quad 0, \quad -1 - \sin\psi)^t \tag{2}$$

$$F(\sigma) = (\sigma'_1 - \sigma'_3) - \sin\Phi'.(\sigma'_1 + \sigma'_3) \tag{3}$$

2.2. *Theoretical expression of the dilatancy*

We use the yielding expression found by Frydman, Zeitlen, and Alpan (1973). In their relation, Frydman et al. assume that the energy dissipated per unit volume during the loading dW^p (Equation (4)) is equal to the energy dissipated by the interparticle slippage in the octahedral plane (Equation (5)) with Φ_μ the mean value of the interparticle angle of friction, with $\varepsilon_m = 1/3.\ (\varepsilon_1 + \varepsilon_2 + \varepsilon_3)$ the first invariant of the strain tensor, with $\varepsilon_d = \frac{1}{3}\sqrt{(\varepsilon_1 - \varepsilon_2)^2 + (\varepsilon_2 - \varepsilon_3)^2 + (\varepsilon_3 - \varepsilon_1)^2}$ the second invariant of the strain tensor, with $\sigma'_{oct} = 1/3.\ (\sigma'_1 + \sigma'_2 + \sigma'_3)$ the first invariant of the stress tensor, with $\tau_{oct} = \frac{1}{3}\sqrt{(\sigma'_1 - \sigma'_2)^2 + (\sigma'_2 - \sigma'_3)^2 + (\sigma'_3 - \sigma'_1)^2}$ the second invariant of the stress tensor

$$dW^p = 3.\sigma'_{oct}.d\varepsilon^p_m + 3.\tau_{oct}.d\varepsilon^p_d \tag{4}$$

$$dW^p = 3.\sigma'_{oct}.tg\Phi_\mu.d\varepsilon^p_d. \tag{5}$$

This allows determination of the relation between the stress and the plastic strain:

$$\frac{\tau_{oct}}{\sigma'_{oct}} + \frac{d\varepsilon^p_m}{d\varepsilon^p_d} = tg\phi_\mu. \tag{6}$$

When failure occurs for the triaxial test, the ratio between the stress is a function of F' the drained friction angle only (Equation (7)), and the ratio between the octahedral stress is now a function of Φ' (Equation (8)):

$$\frac{\sigma'_1}{\sigma'_2} = \frac{1 + \sin\phi'}{1 - \sin\phi'} \tag{7}$$

$$\frac{\tau_{oct}}{\sigma'_{oct}} = \frac{2.\sin\phi'.\sqrt{2}}{3 - \sin\phi'}. \tag{8}$$

The non-associated flow rule (Equation (2)) allows definition of the volumetric plastic deformation and the two main plastic deformations for the triaxial test:

$$d\varepsilon^p_m = \xi(d\varepsilon^p_1 + d\varepsilon^p_2 + d\varepsilon^p_3)/3 = -\xi.2/3.\sin\psi \tag{9}$$

$$\begin{aligned} d\varepsilon_1^p &= \xi.(1-\sin\psi) \\ d\varepsilon_3^p &= d\varepsilon_2^p = \tfrac{1}{2}.(3.d\varepsilon_{oct}^p - d\varepsilon_1^p) = \xi.\tfrac{1}{2}.(-1-\sin\psi) \end{aligned}. \tag{10}$$

The knowledge of the main strain allows the determination of the strain ratio in Equation (11) as a function of Ψ:

$$\frac{d\varepsilon_m^p}{d\varepsilon_d^p} = \frac{-4.\sin\psi}{(3-\sin\psi).\sqrt{2}}. \tag{11}$$

The Frydman relation (Equation (6)) can be used for the plastic behaviour at the failure and can be transformed in a dilatancy equation with the help of Equations (8) and (11), with a direct relation between the three parameters Φ, Ψ and Φ_μ:

$$\frac{2.\sin\phi'.\sqrt{2}}{(3-\sin\phi')} - \frac{4.\sin\psi}{(3-\sin\psi).\sqrt{2}} = tg\phi_\mu. \tag{12}$$

This relation allows us to formulate the dilatancy as a function of the interparticle angle of friction Φ_μ and the friction angle Φ:

$$\sin\Psi = \frac{3.\sqrt{2}\left(\frac{2.\sin\Phi'\sqrt{2}}{3-\sin\Phi'} - tg\Phi_\mu\right)}{4+\sqrt{2}.\left(\frac{2.\sin\Phi'.\sqrt{2}}{3-\sin\Phi'} - tg\Phi_\mu\right)} \tag{13}$$

The relation between dilatancy Y, peak friction angle F, and critical state friction angle F_{cv} was also investigated by Bolton (1986), who proposed the following equation from experimental investigations:

$$0.8\Psi = \Phi' - \Phi_{cv} \tag{14}$$

An expression of the dilatancy was also found by Rowe (1962) (Equation (15)), which can be rewritten as (Equation (16)):

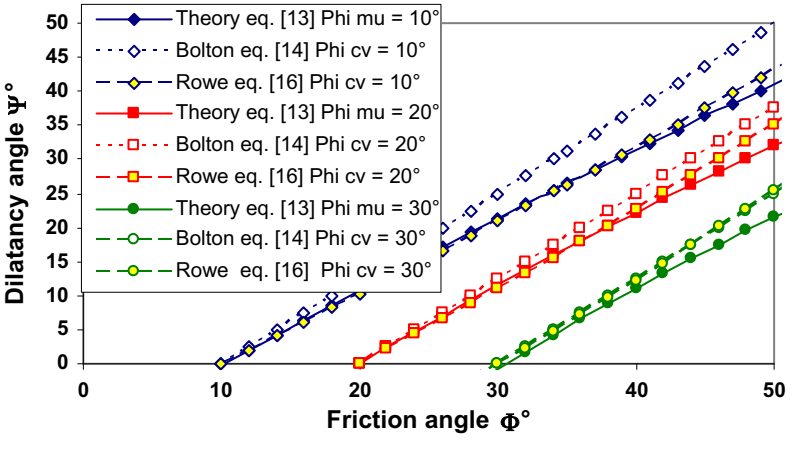

Figure 1. The dilatancy angle as a function of the friction angle for Equation (13) compared with the Bolton expression (Equation (14)) and the Rowe expression (Equation (16)).

$$\frac{1+\sin\Phi'}{1-\sin\Phi'} = \frac{1+\sin\Phi_{cv}}{1-\sin\Phi_{cv}} \cdot \frac{1+\sin\Psi}{1-\sin\Psi} \tag{15}$$

$$\sin\Psi = \frac{\frac{1+\sin\Phi'}{1-\sin\Phi'} \cdot \frac{1-\sin\Phi_{cv}}{1+\sin\Phi_{cv}} - 1}{\frac{1+\sin\Phi'}{1-\sin\Phi'} \cdot \frac{1-\sin\Phi_{cv}}{1+\sin\Phi_{cv}} + 1} \tag{16}$$

In Figure 1 we follow the observation of Frydman et al. (1973), who found the interparticle angle of friction Φ_μ close to the friction linked to the maximum contraction of the triaxial test. Like Negussey, Wijewickreme and Vaid (1987) and Biarez and Hicher (1994), we assume that the angle of maximum contraction is equal to the critical-state friction angle Φ_{cv}. These two angles are different according to Rowe (1962) and Bolton (1986), but they are used here to make an easy comparison between the three relations, so that there is an equality between Φ_μ and Φ_{cv}. Equation (13) is compared with the Bolton Equation (14) and the Rowe Equation (16). It can be seen that the discrepancy between the theoretical dilatancy (Equation (13)) and the Rowe dilatancy (Equation (16)) is less than 4°. The theoretical expression is also close to the experimental expression (Equation (14)) for the current range of the friction angle (Φ: 20–45°) and critical angle (Φ_{cv}: 20–30°) but gives a smaller value of the dilatancy for friction angles Φ larger than 45° and for small critical angle (Φ_{cv}: 10°). Nevertheless, as Equation (13) is found from theoretical point of view and can be used in a three dimensional state of stress, it is chosen for the present study.

2.3. *Equilibrium condition*

The evolution of the main stresses along the radius (Figure 2) exhibits three different states of the soil from the borehole wall to infinity:

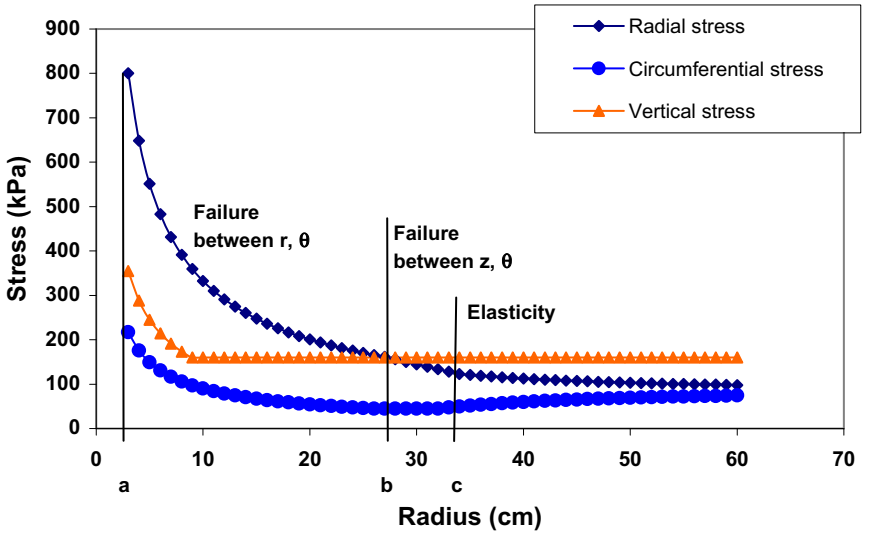

Figure 2. Evolution of the main stresses along the radius and corresponding elasto-plastic areas.

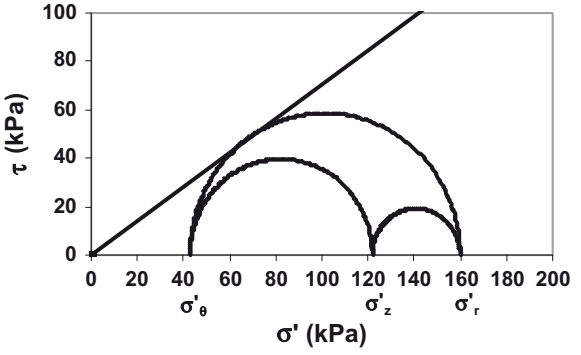

Figure 3. Failure criterion reached in the θ–r horizontal plane at the borehole wall.

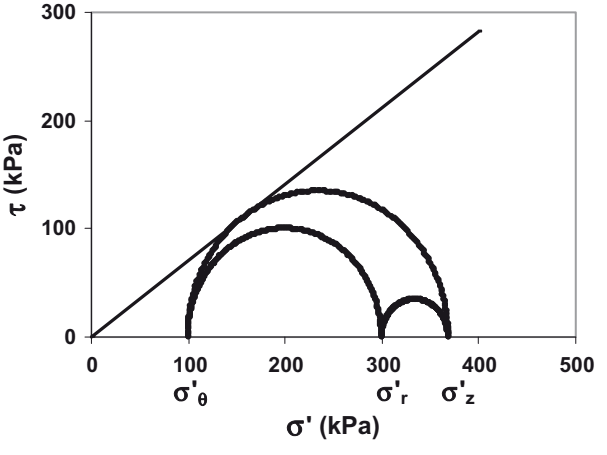

Figure 4. Failure criterion reached in the θ–z vertical plane close to a radius of 34 cm (Figure 2).

- First area: plasticity appears between the radial stress σ'_r and the circumferential stress σ'_θ in the horizontal plane (Figure 3). This first plastic area extends between radius a (borehole wall) and radius b (external radius of the first plastic area).
- Second area: plasticity may also appear in the vertical plane between the vertical stress σ'_z and the circumferential stress σ'_θ (Figure 4) in an area between the radii b and c (external radius of both plastic areas in Figure 2). This result was also found by Wood and Wroth (1977). This area should be extended for a hard soil where the initial differences between the radial and the vertical stress are larger.
- Third area: an elastic equilibrium extends beyond radius c.

The use of fixed angles of dilatation and friction is a simplification and it would be preferable to consider these angles as function of density and pressure. This would, however, result in even more complex mathematics and it is not compatible with the aim of finding simple mechanical characteristics.

In the horizontal plane, the equilibrium of an element of soil is given by Equation (17) and in the vertical plane by Equation (18), with the assumption of a constant pore pressure along the radius σ'_h, σ'_r, σ'_z. Effective circumferential, radial, vertical stresses:

$$\sigma'_r - \sigma'_\theta + r.d\sigma'_r/dr = 0 \tag{17}$$

$$d\sigma'_z/dz = \gamma' \tag{18}$$

2.4. *Equilibrium in the θ–r horizontal plane*

This first plastic area takes place between the borehole radius a, where the pressuremeter probe applies the pressure p and the radius b. The Mohr–Coulomb Equation (3) is used between the radial stress σ'_r (major stress) and the circumferential stress σ'_q (minor stress) and we obtain the ratio N between these two stresses:

$$\sigma'_\theta/\sigma'_r = N \tag{19}$$

$$N = (1 - \sin\Phi')/(1 + \sin\Phi') \tag{20}$$

Equation (19) allows σ'_θ to be found as a function of σ'_r and we can use it in the horizontal equilibrium equation (Equation (17)). This leads to first order differential equation (Equation (21)), which is integrated in Equation (22) between the radius of the borehole a and the current radius r, with the pressure p′ applied at the borehole wall:

$$\sigma'_r - N.\sigma'_r + r.d\sigma'_r/dr = 0 \tag{21}$$

$$Ln\left(\frac{r}{a}\right) = \frac{1}{(N-1)}.Ln\left(\frac{\sigma'_r}{p'}\right). \tag{22}$$

In the same area, the non-associated flow rules (Equation (2)) and the plastic potential (Equation (1)) yield the ratio n between the radial deformation $d\varepsilon_r^p$ and the borehole deformation $d\varepsilon_\theta^p$:

$$d\varepsilon_r^p/d\varepsilon_\theta^p = -n \tag{23}$$

$$n = (1 - \sin\Psi)/(1 + \sin\Psi) \tag{24}$$

Equation (23) can be integrated with a constant C_1 independent of the displacement u and the radius r:

$$\varepsilon_r^p = -n.\varepsilon_\theta^p + C_1 \tag{25}$$

As the elastic part of the deformation is considerably smaller than the plastic deformations it can be neglected. The effect of this simplification should be significant for high angle of friction and low elastic stiffness (Yu & Houlsby, 1991). Eventually, engineering practice shows that hard soils behave with high angle of friction, which is balanced by high elastic stiffness. For soft soil, low elastic stiffness is balanced by a low angle of friction. Then, it is a reasonable common assumption to neglect the elastic part of the deformation, like Hughes et al. (1977) and Gibson and Anderson (1961).

The use of these expressions in Equation (23) with an assumption of small deformation Equation (26) gives a first order differential equation (Equation (27)), which is integrated between the radius of the borehole a and the current radius r in Equation (28):

$$\varepsilon_r = du/dr \quad \varepsilon_\theta = u/r \tag{26}$$

$$du/dr = -n.u/r + C_1 \tag{27}$$

$$Ln\left(\frac{r}{a}\right) = \frac{1}{(n+1)}.Ln\left[\frac{\frac{u_a}{a}.(1+n) - C_1}{\frac{u}{r}.(1+n) - C_1}\right]. \tag{28}$$

Combining Equations (22) and (28) we find the first plastic area condition:

$$Ln\left[\frac{\frac{u_a}{a}.(1+n) - C_1}{\frac{u}{r}.(1+n) - C_1}\right] = \frac{(1+n)}{(1-N)}.Ln\left(\frac{p'}{\sigma'_r}\right) \tag{29}$$

As the limit between the first and the second plastic area is linked to the value of the radial stress being equal to the vertical stress, we obtain the value of b, the external radius of the first plastic area:

$$b = a.\left(\frac{p'}{\sigma'_z}\right)^{\left(\frac{1}{1-N}\right)}. \tag{30}$$

2.5. *Equilibrium in the θ–z vertical plane*

In the second plastic area, the plastic condition gives a relation between the vertical stress σ'_z and the circumferential stress σ'_θ:

$$\sigma'_z = \gamma.z; \quad \sigma'_\theta. = N.\gamma'.z \tag{31}$$

The horizontal equilibrium condition (Equation (17)) gives the relation between the stress at the current radius r and the stress at the limit c between the last plastic zone and the elastic zone:

$$\frac{r}{c} = \frac{(N.\gamma'.z - \sigma'_{rc})}{(N.\gamma'.z - \sigma'_r)}. \tag{32}$$

The plasticity condition shows that the radial deformation $d\varepsilon_r$ is not concerned by the flow rule and can be integrated with constants C_2 and C_3:

$$\varepsilon_r = du/dr = C_2; \quad u = C_2.r + C_3. \tag{33}$$

From Equations (32) and (33) we obtain the second plastic area condition:

$$\frac{u - C_3}{u_c - C_3} = \frac{(N.\gamma'.z - \sigma'_{rc})}{(N.\gamma'.z - \sigma'_r)} \tag{34}$$

An elastic area is assumed beyond the larger plastic radius.

2.6. Global equilibrium with two plastic areas

The continuity of stress between the three different areas allows the evaluation of C_1:

$$C_1 = \frac{n.\left(\frac{u_a}{a}\right).(1+n).\left(\frac{\gamma.z}{p}\right)^{\delta} + (1+n).(N-K_0).\frac{\gamma.z}{2.G}}{1+n.\left(\frac{\gamma.z}{p}\right)^{\delta}} \tag{35}$$

$$\delta = \frac{1+n}{1-N}. \tag{36}$$

We obtain the general relation condition between stress and deformation, which is the general form of the pressuremeter equation with two plastic areas:

$$Ln\left[\frac{u_a}{a}.(1+n) - C_1\right] = \delta.Ln(p) - \delta.Ln(\gamma.z) + Ln\left[(1-K_0).\gamma.z.\frac{(1+n)}{2.G} - C_1\right] \tag{37}$$

The value of coefficient C_1 is usually close to a hundredth of the the borehole deformation. For example, with the mean values of the numerical analysis (Table 1) and for an applied pressure of 500 kPa, with a borehole deformation of 4.27×10^{-2}, the value of C_1 is -1.45×10^{-3}, which is –3.4% of the radial deformation. This is very small and can be neglected, and leads to a linear relation between the logarithm of the borehole deformation at the borehole wall and the pressure applied by the pressuremeter. The proportionality between these two variables was first shown by Hughes et al. (1977) with the use of Rowe's dilatancy theory. Such a relation allows the determination of the slope δ of the straight line between the variables, which is a function of ϕ' the angle of internal friction, and Φ_μ the interparticle angle of friction. Knowledge of Φ_μ and δ leads to Φ' the angle of internal friction of the soil in a unique and accurate determination.

2.7. Global equilibrium with only one plastic area

The continuity of stress between the two different areas leads to:

$$C_1 = \frac{K_0.\gamma.z.(1-N).(n-1)}{2.G.(1+N)} \tag{38}$$

The general condition between stress and deformation, which is the general form of the pressuremeter equation for one plastic area, is then:

Table 1. Mechanical parameters.

	Carter's model	Model presented here
c (kPa)	0	0
Φ(°)	40	40
Φ_μ(°)		32.3
ψ(°)	10	10
E (kPa)	65,000	65,000
ν(kPa)	0.3	0.3
k	1	

$$Ln\left[\frac{u_a}{a}.(1+n)-C_1\right]=\delta.Ln(p)-\delta.Ln\left[\frac{2.K_0.\gamma.z}{(1+N)}\right]+Ln\left[K_0.\gamma.z.\frac{(1-N).(1+n)}{2.G.(1+N)}-C_1\right] \quad (39)$$

The proportionality between the borehole deformation at the borehole wall and the pressure applied by the pressuremeter is also obtained.

The difference between the two cases is linked to the value of the radial stress at the radius of the external area of plasticity c. For a single plasticity between r and θ, the value of the radial stress must be larger than the vertical stress $\sigma'_{rc} > \sigma'_z$ and this leads to the Wood and Wroth (1977) condition between K_0 and Φ':

$$K_0 \geqslant \frac{1}{(1+\sin\phi')} \quad (40)$$

2.8. Threshold plastic pressure, two plastic areas

The theoretical threshold plastic pressure is obtained when the radial stress (a case with two plastic areas) or the circumferential stress (a case with one plastic area) exceed the limit so that the soil exhibits plasticity. Putting the value of N.γ.z for the circumferential stress into the equation of elastic behaviour, we obtain the radial stress, which is the theoretical threshold plastic pressure:

$$p'_f = (2.K_0 + N).\gamma' z. \quad (41)$$

2.9. Threshold plastic pressure, one plastic area

The value of the radial stress when plasticity is initiated, leads to the theoretical threshold plastic pressure:

$$p'_f = (1+\sin\Phi').K_0.\gamma'.z, \quad (42)$$

which was first obtained by Baguelin et al. (1978).

2.10. Conventional limit pressure, two plastic areas

For the two cases, we can find the conventional limit pressure p_l when we assume that the volume of the probe is double the initial volume. The borehole deformation at the borehole is then equal to $\sqrt{2}-1$. This pressure can be directly measured with the pressuremeter whereas the theoretical limit pressure is expressed as an infinite expansion and cannot be directly measured.

This particular value of the borehole deformation is put into Equation (37) and we obtain the conventional limit pressure:

$$p'_l = \gamma.z.\left(\frac{\left[(1+n).(\sqrt{2}-1)-C_1\right].2.G}{[(1-K_0).(1+n).\gamma'.z-2.G.C_1]}\right)^{(1/\delta)} \quad (43)$$

This relation is quite different from the one proposed by the 'Comité Technique Régional Européen 4' (CTRE4) edited by Amar, Clarke, Gambin, and Orr (1991), which is based on Ménard experimental correlations.

$$p'_l = 250.\left[2^{\left(\frac{\phi-24}{4}\right)}\right] + K_0.\gamma.'z \tag{44}$$

The Ménard relation was derived from many pressuremeter tests. Theoretical considerations show that the main shearing takes place between the radial stress σ'_r and the circumferential stress σ'_θ, which lie in the horizontal plane. For the pressuremeter test the vertical stress increases with the depth. The shearing applied by the pressuremeter probe begins at a value of zero when the radial stress at the borehole wall is equal to the at-rest horizontal pressure and increases until a maximum when the limit pressure is reached. The maximum shearing applied to the soil is linked to the difference between the limit pressure and the horizontal at-rest pressure p_0. The value of p_0 increases with the depth, so the value of the maximum shearing applied by the pressuremeter should increases with the depth. The value of the mean stress in the Mohr–Coulomb plane is equal to the sum of the radial stress, or limit pressure, and the circumferential stress. This sum is proportional to the radial stress. The ratio between the shearing stress and the mean stress should be proportional to the friction angle for a granular soil. This gives a condition of proportionality between the limit pressure and the vertical stress, which is obtained from Equation (43). The Ménard equation (Equation (44)) seems to fit these considerations only for a mean depth close to 12 m. For a test close to the surface, it seems to underestimate the friction angle, and for a very deep test it seems to overestimate the friction angle. Futhermore, the Ménard relation does not take into account the nature of the soil, and the variation of the interparticle angle of friction. It overestimates friction angle for loams, which have lower interparticle angle of friction than sands and gravels.

Other authors proposed an expression of the limit pressure, e.g. Carter et al. (1986) in Equation (45), but these equations relate to an infinite expansion of the radius, which is never measured, whereas the proposed expression relates to a conventional expansion of the probe, twice the initial volume, which can be directly measured. The proposed expression allows the conventional limit pressure p_L to be found directly without any numerical iterative process as needed for the equation of Carter et al. (1986) (Equation (45)) which uses numerical resolution. Furthermore Equation (45) gives an inverse proportionality between the limit pressure and the horizontal pressure at rest p_0, which is a contradiction to an assumed increasing of the limit pressure as a function of the depth for a granular soil.

$$T.\left(\frac{p_L}{\sigma_R}\right)^{\gamma} - Z.\left(\frac{p_L}{\sigma_R}\right) = \frac{2.G}{p_0}.\frac{N+1}{N-1} \tag{45}$$

2.11. Conventional limit pressure, one plastic area

The particular value of the borehole deformation $\sqrt{2}-1$ is put into Equation (39), which leads to the value of the conventional limit pressure:

$$p'_l = \frac{2.K_0.\gamma.z}{(1+N)}.\left(\frac{[(1+n).(\sqrt{2}-1)-C_1].2.G.(1+N)}{K_0.\gamma'.z.[(1-N).(1+n)-2.G.C_1.(1+N)]}\right)^{(1/\delta)} \tag{46}$$

It appears that the conventional limit pressure is proportional to the vertical stress.

3. Application of the proposed method

3.1. Experimental study

Full-scale pressuremeter tests were performed by Manassero (1989) in a calibration chamber, on dry Ticino sand. The specimen measured 1.2 m in diameter and 1.5 m in height. In a first step, it was subjected to one-dimensional vertical loading. In a second step, pressuremeter tests were carried out under controlled boundary conditions. The pressuremeter probe was the Camkometer apparatus, and 21 tests were carried out on a relative density between 42.2% and 92.3%. The overconsolidation ratio (OCR) was from 1 to 7.7. The results for the test 228 (D_r = 77%, OCR = 5.5) are shown in Figures 5 and 6.

3.2. Calibration of the mechanical parameters

The elastic parameters of the test are chosen on the initial elastic part of the loading, for a pressure lower than the creep pressure which should be equal to 338 kPa. With a Poisson's ratio assumed to be 0.3, the Young modulus of the sand is 65,000 kPa for an elastic slope of the loading (Figure 5) identical to the experimental one. The mechanical parameters used are shown in Table 1.

The friction angle is chosen to be the mean value obtained by Silvestri (2001) on this test, which is 40°. The dilatancy angle is chosen to be 10° as measured by Manassero (1989) on this sand. The parameter k is 1 for the Carter model related to a cylindrical expansion. The interparticle angle of friction ϕ_μ is chosen to be 32.3° so that the use of Equation (13) allows the same dilatancy angle ψ to be found for the two theories. This interparticle angle of friction is 1.7° smaller than the value of the 34° of the critical void ratio angle Φ_{cv} reported by Silvestri (2001), which is considered to be an acceptable difference.

The horizontal and vertical stress are fixed to the experimental initial value reported by Silvestri (2001), i.e. 200 kPa.

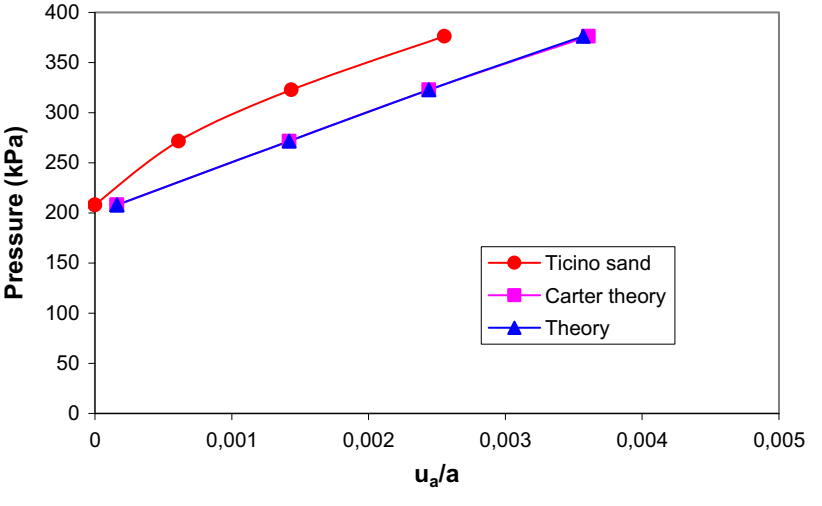

Figure 5. Calibration of the elastic parameters of the Carter theory and the theory presented in this paper.

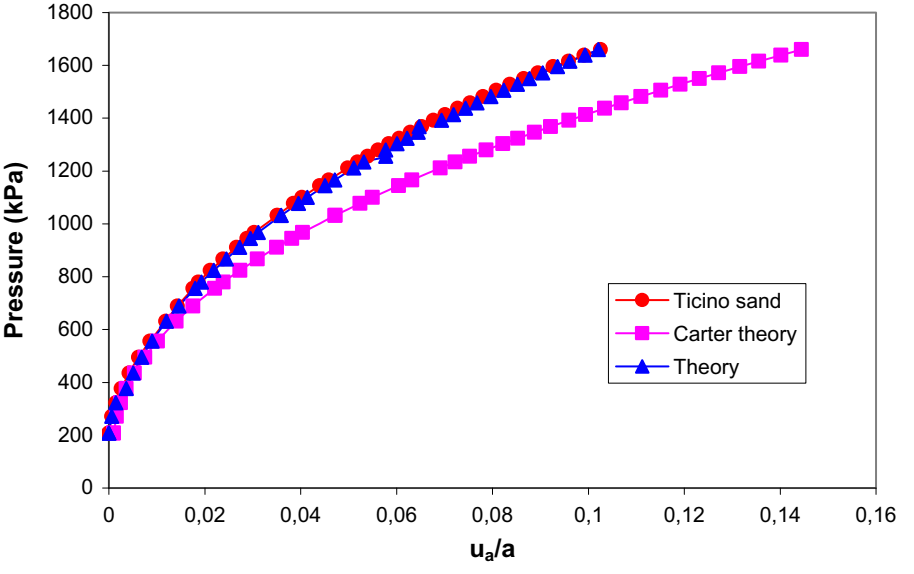

Figure 6. Comparison between experimental data on Ticino sand, the Carter et al. (1986) theory and presented model.

3.3. *Comparison between experimental and theoretical curves*

The theory proposed by Carter et al. (1986) is used here with the parameters given in Table 1 and the condition of stress presented previously. It appears (Figure 6) that this theory gives a larger strain than that observed by Manassero (1989).

For the same parameter set, the proposed model (Figure 6) finds a small discrepancy between the experimental and theoretical deformations and validates on this test the presented theory.

4. Conclusion

We have presented a theoretical study of the interpretation of the pressuremeter test. This new theory takes into account the vertical and the horizontal non-standard elasto-plastic equilibrium around the pressuremeter probe. Plastic behaviour is assumed between the radial stress and the circumferential stress and also between the vertical stress and the circumferential stress.

The analysis shows that four mechanical parameters and the vertical stress have an influence on the pressuremeter results for a granular soil (shearing modulus, friction angle, interparticle angle of friction and coefficient of at rest pressure). The use of this new theory on a pressuremeter test performed by Manassero (1989) shows a very small discrepancy between theoretical and experimental results. This allows validation of this theory for the pressuremeter test on sand.

References

Allouani, M., Cambou, B., & Dubujet, P. (1995). Influence of the compressibility-dilatancy models on the result of a pressuremeter test. *4th International Symposium, The Pressuremeter and its New Avenues* (pp. 57–63), Université de Sherbrooke, G. Ballivy Editor, A.A. Balkema, Rotterdam.

Amar, S., Clarke, B.G.F., & Gambin, M., Orr, T.L.L. (Eds.). (1991). The application of pressuremeter test results to foundation design in Europe. *Comité Technique Régional Européen 4, Pressiomètre* (pp. 1–24). A.A. Balkema Editor, Rotterdam.

Baguelin, F., Jezequel, J.F., Le Mee, E., & Le Mehauté, A. (1972). Expansion of cylindral probes in cohesive soils. *ASCE Soil Mechanics, 11*, 1129–1142.

Baguelin, F., Jezequel, J.F., & Shields, D.H. (1978). The pressuremeter and foundation engineering. *Trans Tech Publication editor*, Clausthal, Germany, p. 615.

Bahar, R., Cambou, B., Labanieh, S., & Foray, P. (1995). Estimation of soil parameters using a pressuremeter test. *4th International Symposium, The Pressuremeter and its New Avenues* (pp. 65–72) Université de Sherbrooke, G. Ballivy Editor, A.A. Balkema, Rotterdam.

Biarez, J., & Hicher, P.Y. (1994). *Elementary mechanics of soils behaviour, saturated remoulded soils*. Rotterdam: Balkema.

Bolton, M.D. (1986). The strength and dilatancy of sand. *Geotechnique, 36*, 65–77.

Cambou, B., & Bahar, R. (1993). Utilisation de l'essai pressiométrique pour l'identification de paramètres intrinsèques du comportement du sol. *Revue Française de Géotechnique, 63*, 39–50.

Carter, J.P., Booker, J.R., & Yeung, S.K. (1986). Cavity expansion in cohesive frictional soils. *Geotechnique, 36*, 349–358.

Cassan, M. (2005). Les essais pressiométriques et leur applications en France. Rappels historiques et état des connaissances. *International Symposium Pressio 2005* (pp. 125–200), Vol. 2, M. Gambin, J.P. Magnan, P. Mestat editors, Presses Ponts et Chaussées, Paris.

Clarke, B.G. (1996). Pressuremeter testing in ground investigation, Part I: Site operations. *Geotechnical Engineering, 119*, 96–108.

Clough, G.W., Briauld, J.L., & Hughes, J.M.O. (1990). The development of pressuremeter testing. *3rd International Symposium on Pressuremeters* (pp. 25–45) University of Oxford, G.T. Houls by Editor, Thomas Telford.

Dalton, C. (2005). United Kingdom experience with pressuremeter 1982–2005, *International Symposium Pressio 2005* (pp. 201–210), Vol. 2, M. Gambin, J.P. Magnan, P. Mestat editors, Presses Ponts et Chaussées, Paris.

DTU 13-12. (1988). *Règles pour le calcul des foundations superficielles, AFNOR DTU P 11-711*, Cahiers du Centre Scientifique et Technique du Bâtiment, Paris.

Durkee, D.B., Langer, J.A., Hughes, J.M.M., & Smith, D.E. (2005). Pressuremeter tests in sand gravel and cobbles. *International Symposium Pressio 2005* (pp. 601–609), Vol. 1, M. Gambin, J.P. Magnan, P. Mestat editors, Presses Ponts et Chaussées, Paris.

Fahey, M. (1986). Expansion of a thick cylinder of sand: a laboratory simulation of the pressuremeter test. *Geotechnique, 36*, 397–424.

Fahey, M. (2005). Stiffness of sands of differents ages from pressuremeter and seismic cone tests in Perth. *International Symposium Pressio 2005* (pp. 611–619), Vol. 1, M. Gambin, J.P. Magnan, P. Mestat editors, Presses Ponts et Chaussées, Paris.

Fahey, M., & Carter, J.P. (1992). A finite element study of the pressuremeter test in sand using a nonlinear elastic plastic model. *Canadian Geotechnical Journal, 30*, 348–362.

French Standard NF P 94-110. (2000). *Essai pressiométrique Ménard*. AFNOR, Paris.

French Standard NF P 94-250-1. (1996). *Eurocode 7 Calcul géotechnique*. AFNOR, Paris.

Frydman, S., Zeitlen, J.G., & Alpan, I. (1973). The yielding behaviour of particulate media. *Canadian Geotechnical Journal, 10*, 341–362.

Gambin, M. (1990). The history of pressuremeter practice in France. *Third International Symposium on Pressuremeters* (pp. 5–24), University of Oxford, G.T. Houls by Editor, Thomas Telford.

Gibson, R.E., & Anderson, W.F. (1961). In situ measurement of soil properties with the pressuremeter. Civil Engineering and Public Works Review, Vol. 56, N° 658 May, 615–618.

Hughes, J.M.O., Wroth, C.P., & Windle, D. (1977). Pressuremeter tests in sand. *Geotechnique, 27*, 455–477.

Jewell, R.J., Fahey, M., & Wroth, C.P. (1980). Laboratory studies of the pressuremeter test in sand. *Geotechnique, 30*, 507–531.

Juran, I., & Beech, J.F. (1986). Effective stress analysis of soil response in a pressuremeter test. The pressuremeter test and its marine application. *Second international symposium on Pressuremeters, Texas A&M University, College Station, J.L. Briaud, J.M. Audibert Editors, ASTM Special Technical Publication, 950*, 150–168.

Juran, I., & Mahmoodzadegan, B. (1989). Interpretation procedure for pressuremeter in sand. *Journal of Geotechnical Engineering, ASCE, 115*, 1617–1632.

Levasseur, S., Malecot, Y., Boulon, M., & Flavigny, E. (2010). Statistical inverse analysis based on genetic algorithm and principal component analysis: application to excavation problems and pressuremeter test. *International Journal for Numerical and Analytical Methods in Geomechanics, 34*, 471–491.

Manassero, M. (1989). Stress-strain relationship for drained self-boring pressuremeter tests and large in-situ plate tests in London clay. *Geotechnique, 27*, 217–243.

Ménard, L. (1975). The interpretation of pressuremeter test results. *Sols Soils,* Vol. 26, 1–43, Paris.

Monnet, J. (1990). Theoretical study of elasto-plastic equilibrium around pressuremeter in sands. *3rd International Symposium on Pressuremeters* (pp. 137–148), University of Oxford, G.T. Houls by Editor, Thomas Telford.

Monnet, J., & Allagnat, D. (2002). Design of a large soil retaining structure with pressuremeter analysis. *Geotechnical Engineering, 155*, 71–78.

Monnet, J., & Allagnat, D. (2006). Interpretation of pressuremeter results for the design of diaphragm wall. *Geotechnical Testing Journal, ASTM, 29*, 126–132.

Monnet, J., Allagnat, D., Teston, J., Billet, P., & Baguelin, F. (2006). Foundation design of a large arch bridge on alluvial soils. *Geotechnical Engineering, 159*, 19–28.

Monnet, J., & Khlif, J. (1994). Etude théorique et expérimentale de l'équilibre élasto-plastique d'un sol pulvérulent autour du pressiomètre. *Revue Française de Géotechnique, 67*, 3–12.

Negussey, D., Wijewickreme, W.K.D., & Vaid, Y.P. (1988). Constant-volume friction angle of granular materials. *Canadian Geotechnical Journal, 25*, 50–55.

Obrzud, R.F., Vulliet, L., & Truty, A. (2009). A combined neural network/gradient-based approach for identification of constitutive model parameters using self-boring pressuremeter tests. *International Journal for Numerical and Analytical Methods in Geomechanics, 33*, 817–849.

Rowe, P.W. (1962). The stress dilatancy relation for static equilibrium. Proceedings of the Royal Society London A, 269, 500–527, London.

Rowe, P.W. (1969). The relation between the shear strength of sands in triaxial compression, plane strain and direct shear. *Geotechnique, 19*, 75–86.

Silvestri, V. (2001). Interpretation of pressuremeter tests in sand. *Canadian Geotechnical Journal, 38*, 1155–1165.

Wood, D.M., & Wroth, P.C. (1977). Some laboratory experiments related to the results of pressurementer tests. *Geotechnique, 27*, 181–201.

Yu, H.S., & Houlsby, G.T. (1991). Finite cavity expansion in dilatant soils: loading analysis. *Geotechnique, 41*, 173–183.